Environmental Science and Pollution Research (2021) 28:27731–27741
https://doi.org/10.1007/s11356-021-12343-9

RESEARCH ARTICLE

The role of rhizofiltration and allelopathy on the removal of cyanobacteria in a continuous flow system

Ana Teresa Castro-Castellon[1,2] · Jocelyne Mary Rose Hughes[3] · Daniel Steven Read[4] · Yaldah Azimi[1] · Michael James Chipps[5] · Nicholas Peter Hankins[1]

Received: 30 September 2019 / Accepted: 2 January 2021 / Published online: 30 January 2021

Abstract

A continuous flow filtration system was designed to identify and quantify the removal mechanisms of Cyanobacteria (*Microcystis aeruginosa*) by hydroponic biofilters of *Phalaris arundinacea* compared to synthetic filters. The filtration units were continuously fed under plug-flow conditions with *Microcystis* grown in photobioreactors. *Microcystis* cells decreased at the two flow rates studied (1.2 ± 0.2 and 54 ± 3 cm^3 min^{-1}) and results suggested physical and chemical/biological removal mechanisms were involved. Physical interception and deposition was the main removal mechanism with packing density of the media driving the extent of cell removal at high flow, whilst physical and chemical/biological mechanisms were involved at low flow. At low flow, the biofilters decreased *Microcystis* cell numbers by 70% compared to the controls. The decrease in cell numbers in the biofilters was accompanied by a chlorotic process (loss of green colour), suggesting oxidative processes by the release of allelochemicals from the biofilters.

Keywords Biofilters · Biofiltration · *Phalaris arundinacea* · Allelopathy · Cyanobacteria removal · *Microcystis* removal · Responsible Editor: Vitor Manuel Oliveira Vasconcelos

Introduction

Eutrophication affects inland and marine waters worldwide since the boom of intensive agriculture practices after the Second World Word with typical manifestations of algal (algae and cyanobacteria) blooms (Le Moal et al. 2019; Qin et al. 2019). Water scarcity leading to shortages of potable water due to climate change is a reality (Flörke et al. 2018). Furthermore, toxic algal blooms frequency will continue to increase with rising temperatures due to climate change (Chorus and Bartram 1999; Huisman et al. 2018). Not only do algal blooms threaten water quality with significant economic, biologic and public health consequences (Martinez Hernandez et al. 2009; Hudnell 2010; O'Neil et al. 2012; Ger et al. 2014; Otten and Paerl 2015) but they can cause significant process disruption and reduce output from water treatment works (WTW) up to 25% by interfering/clogging downstream processes (coagulation, slow sand, and rapid gravity filtration) (Lu et al. 2014). Chemical algicides can be effective to control algal blooms but most are damaging for the environment (Jancula and Marsalek 2011; Fan et al. 2013).

Green technologies are widely used for wastewater and water reuse (Headley and Tanner 2012) but are less frequently used to remediate eutrophication in reservoirs used for recreational or drinking water purposes (Murray et al. 2010). Field-scale biofilters based on plant rhizofiltration of high surface area are used to absorb nutrient or metals from wastewaters (Dushenkov et al. 1995; Raskin and Ensley 2000). The Living-Filter, a floating constructed treatment wetland, was used in a surface reservoir to successfully reduce algal biomass prior to the treatment works for production of potable water (Castro-Castellon et al. 2016). That said, observations from field monitoring provide

Responsible editor: Vitor Manuel Oliveira Vasconcelos

✉ Ana Teresa Castro-Castellon
a.castro-castellon@bathspa.ac.uk

[1] Department of Engineering Science, University of Oxford, Parks Road, Oxford OX1 3PJ, UK

[2] Present address: School of Science, Bath Spa University, Newton Park, Newton St Loe, Bath BA2 9BN, UK

[3] School of Geography and the Environment, University of Oxford, South Parks Road, Oxford OX1 3QY, UK

[4] Centre for Ecology & Hydrology, Wallingford, Oxford OX10 8BB, UK

[5] Thames Water Innovation, Thames Water Utilities Ltd., Reading, UK

valuable ecological data to generate hypotheses to be tested at the bench-scale (Benton et al. 2007).

Bench-scale rhizofiltration studies have been limited to nutrient/metal uptake. Marchand et al. (2014) combined plants and biofilms for metal removal using planted and unplanted Biorack™ to increase copper uptake rate. Kurzbaum et al. (2012) separated the role of the roots and the associated biofilm for the removal of pollutants in a hydroponic system, whilst Weiss et al. (2014) used recirculating metal-rich flows to investigate the effect of water flux through hydroponic roots on metal removal. Removal mechanisms of cyanobacteria by biofiltration processes have not been studied before.

In this study, filtration units of hydroponically developed *Phalaris arundinacea* (biofilters) and synthetic filters of plastic material were used in a novel set-up under continuous flow conditions to study cyanobacteria (*Microcystis aeruginosa*) cell removal by deposition throughout the filter media (depth filtration). The aim of this study was to determine the interactions of *Microcystis* cells with each type of filter, and to understand how the inflow associated with *Microcystis* cells is processed by the filter media. The outcome of this work will provide insights to improve future designs of field-scale Living-Filters promoting the use of green technologies in eutrophic waters.

Materials and methods

Operational system

An experimental mesocosm was set up to test if hydroponically developed roots can be used in an in-reservoir pre-treatment process for removing cyanobacteria from the inflow prior to the water treatment works. The mesocosm system consisted of triplicate filter units with three types of filter media: one biofilter (i.e. *Phalaris arundinacea* roots) and two synthetic monofilament filters (i.e. plastic three-dimensional mesh). In addition, control units with no filter media were included. *Microcystis aeruginosa 1450/3* was obtained from Culture Collection of Algae and Protozoa (CCAP) (hereafter *Microcystis*) and was cultured in photobioreactors and later mixed with dechlorinated water to constitute the feed, which was pumped to the filter and control units. The schematic of the mesocosm set-up is displayed in Fig. 1.

The filtration units (0.32 m L × 0.104 m W × 0.11 m H) were designed in collaboration with Tuan Ta Ltd., London, UK, and made of acrylic transparent material with an internal perforated plate placed at 0.05 m from the inlet. The units were operated in plug-flow mode, with water supplied from an air-mixed 120-L high-density polyethylene tank through nine lines of Marprene long life flexible tubing (1.6 × 1.6 mm). The inflow was controlled by nine pump cassettes in three peristaltic pumps (Watson-Marlow Series 500 × 2 and a Series 325).

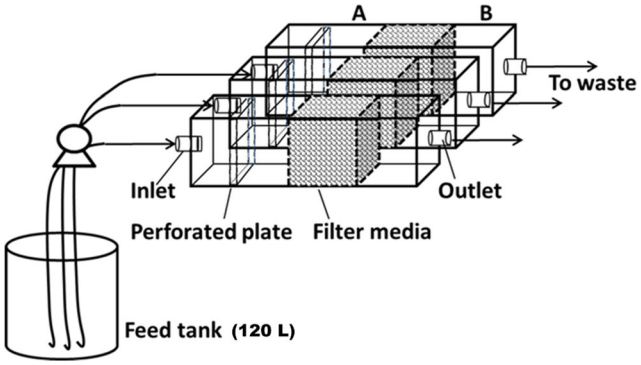

Fig. 1 Schematic of the mesocosm set-up showing the feed tank (120 L) and only three filtration units (3 L each). Top unit with sampling points, where A = upstream and B = downstream of the filter; bottom unit showing inlet and outlet of the units, the perforated plate, and the position of the filter media

Hydraulic configuration of the filtration units

Two flow velocities were chosen for running the experiments. A high flow rate (54 ± 3.0 cm^3 min^{-1}) with a filtration rate of ~ 0.29 m h^{-1} was chosen to resemble the range of filtration rates for slow sand filters (0.3–0.6 m h^{-1}) as slow sand filtration is an effective ecological process in supply water treatment (Campos et al. 2002). A low flow rate (1.3 ± 0.2 cm^3 min^{-1}) was chosen to investigate whether deposition mechanisms could take place in the filter media. Laminar flow in the system becomes mixed in contact with the filter media. The hydraulic properties of the system are summarized in Table 1.

Fluid flow of *Microcystis* cells through biological and synthetic filter media

Three types of filter media were compared: the living roots of hydroponically grown *Phalaris arundinacea* and two synthetic monofilament fabrics with different packing density (fabric1 and fabric2). The packing density for the filter media was estimated from Eq. (1):

$$\text{Packing density} = \text{volume occupied by roots or fabric/total volume } (10\ \text{cm}^3) \quad (1)$$

Stainless steel cages (10 cm^3) were made to contain the biofilters and synthetic media, and empty cages were placed in the control units. The wire diameter was 1.1 mm with an aperture width of 14 mm.

Biofilters: hydroponic growth of *Phalaris arundinacea*

Seeds of *Phalaris arundinacea*, a species from the Poaceae family known as Reed Carnary Grass, were obtained from British Wildflower Plants, Norfolk, UK, and cultivated in sterile coconut coir pellets. After 2 weeks, the roots of plantlets were rinsed, rolled up individually in strips of foam, and

Table 1 Hydraulic properties of the filter units

Experimental flow	Cross-sectional area (m^2)	Volume (m^3)	$V=Q/A$ ($m\ h^{-1}$)	Q ($cm^3\ h^{-1}$)	HRT = Vol/Q (s)
Low	1×10^{-2}	3.3×10^{-3}	0.005	60	2.008×10^{-5}
High	1×10^{-2}	3.3×10^{-3}	0.29	3.3×10^{-3}	3.3×10^{-3}

V, velocity; *Q*, discharge; *HRT*, hydraulic retention time; *Vol*, volume

transferred to 50 cm^3 Falcon™ tubes. To maximize the production of hairy roots, the plantlets were cultured hydroponically in Hoagland's solution at 50% concentration. The tubes were inserted with a hollow plastic straw to facilitate gas interchange and the supply of the solution, and were refilled every 3/4 days. The plants were placed in a growing tent (1.5 m H × 1 m W × 1 m D) equipped with two blue 125 watts compact fluorescent lamps (CFL) and a Sun Mate Grow CFL reflector. The photoperiod was adjusted to a 10:14-h light/darkness cycle (Conn et al. 2013). The photosynthetic active radiation (PAR) of 40 μmol photons $m^{-2}\ s^{-1}$ (30–45 μmol photons $m^{-2}\ s^{-1}$ is recommended) was measured with a terrestrial quantum sensor LI-190SA and light meter LI-250A (Li-Cor International, Ltd., UK). The tubes were covered individually with aluminium foil to prevent light damage to the roots.

After 10 weeks, 48 plants (roots 8–10 cm length) in sets of 16 were placed on top of the stainless steel cages and transferred to 2.1-L tanks. The root biovolume was estimated by rolling them into a plasticized sheet forming a cylinder, and the cylinder's volume was calculated and recorded (Faulwetter et al. 2009).

Synthetic filter media: two types of monofilament nonwoven plastic material

The synthetic filtration media (polyamide nylon) consisted of two types of monofilament nonwoven plastic material of different packing density. These synthetic media were tested to compare their filtration removal efficiencies for *Microcystis* with that of the biofilters. The plastic monofilament layers are bonded by heat to create a sheet of fabric. Differences in flexibility that exist between fabric1 and fabric2 are based on the diameter of the filaments and the number of filament layers that create the sheet of fabric. The filament diameter of fabric1 and fabric2 is 0.5 and 0.03 mm, respectively. Fabric1 is a two-layered filament sheet of 0.8 mm thickness and fabric2 is a multi-layered filament sheet of 1.8 mm thickness. Six stainless steel cubic cages (10 cm^3) were made to contain the fabrics, which were cut in squares of 10 cm^2 (10 cm × 10 cm). Three cages used for fabric1 were tightly filled with 15 pieces each and another three cages for fabric2 were filled with six squares each. The pieces were placed in the cages with the largest surface area facing the direction of the flow. New cages were made and fabric cut for each flow experiment.

Photobioreactors for growing *Microcystis*

*Microcystis w*as cultured in BG11 (modified by Rippka et al. 1979). Aseptic techniques and materials were used throughout the experiment. Four 150 cm^3 sterile flasks each with 50 cm^3 media were spiked with 1 cm^3 of the *Microcystis* stock culture and kept on the bench under fluorescent laboratory lights providing photosynthetic active radiation (PAR) of 10 μmol photons $m^{-2}\ s^{-1}$ (recommended by the CCAP) (Imai et al. 2008). The flasks were shaken manually every 3–4 days and tested weekly for contamination prior to adding 10 cm^3 of fresh media, maintaining *Microcystis* at the exponential growth phase. An aliquot of 5 cm^3 of the *Microcystis* suspension was used as inoculum to grow larger quantities in photobioreactors. The photobioreactors consisted of 1-L Duran bottles, placed in an open water bath with a thermostat keeping the temperature at 22 ± 1 °C. The bottle mouth was closed with a sterile foam plug covered with aluminium foil. To the initial volume of 300 cm^3, 200–250 cm^3 of BG11 was added weekly up to 1 L. Air was diffused into the solutions at a rate of 0.1–0.4 L min^{-1} with a daily cycle (12:12 on/off) divided into four intervals. An additional fluorescent lamp provided a range of 35 μmol photons $m^{-2}\ s^{-1}$ to the closest photobioreactors and a minimum of 10 μmol photons $m^{-2}\ s^{-1}$ to the furthest, and the photoreactors were rotated weekly.

Quality control was conducted by assessing microscopic morphology of *Microcystis* cells and conducting triplicates of cell counts from each bioreactor on a haemocytometer at × 400 magnification using an inverted microscope (Imai et al. 2008). *Microcystis* culture optical density (O.D) was measured in triplicates at $O.D_{620}$ and $O.D_{750}$ nm (Vézie et al. 2002; Dagnino et al. 2006) in a Shimadzu 1800-UV spectrophotometer. To ensure measurable changes in the bioreactors, a minimum $O.D_{620}$ was estimated to be 0.3 (~ 6.5×10^{-6} cells $cm^{3\ -1}$) with the resulting calibration Eq. (2):

$$Y = 1E + 07x + 504384 \quad (2)$$

To ensure there was no bacterial growth monitoring, changes at $O.D._{750nm}$ were conducted.

Microcystis as the particles in suspension

Microcystis cells are spherical particles with an average size of 3.2 μm ± 0.8 μm ($n = 30$), obtained under light microscope (Eclipse E-200 Nikkon). Cells that were in division, representing approximately 20% of the cell population, were also included in the average size.

An increase in the concentration of *Microcystis* cells is expected upstream of the filter media (see Fig. 1). The particle concentration in plug-flow mode can be expressed as a dimensionless parameter, which represents the ratio of the particle concentration upstream of the filter media relative to the inflow to the filtration unit following Eq. (3),

$$\text{Cumulative mass fraction (CMF)} = C_m/C_f \quad (3)$$

where CMF is the cumulative mass fraction; C_m is the concentration of cells on the upstream side of the filter at sampling point A (Fig. 1), and C_f is the concentration of cells in the inflow upstream of the filter unit at the inlet (Fig. 1). This parameter will indicate the filtration mode of the filter media (US-EPA 2005). Hence CMF = 1 indicates an operating system in deposition mode. The cells are moving with the inflowing water at a steady rate before passing through the filter media. CMF ≥ 1 indicates there is a scouring force applied tangentially upstream to the media, and CMF ≤ 1 suggests the system operates in deposition filtration mode.

Microcystis cell count with flow cytometry

Microcystis cell concentration was first estimated by manual counting on a haemocytometer at × 400 magnification on an inverted microscope. The large number of samples generated and the poor count discrimination of low O.D readings (< 0.015) led to the use of flow cytometry for subsequent cell counts using a BD Accuri C6 (BD Biosciences, UK).

The fluidic system in the instrument is designed so that the suspended cells in the sample are delivered one by one to a specific point with the illuminating beam. The velocity of the samples loaded into the channel was set at 35 μl min^{-1}. The instrument measures the light scattered by the cells at right angles to the laser beams (called side scatter, SS) and light scattered in a forward direction (forward scatter, FS). The size and shape of the cells affects the forward scatter whilst small structures (internal or external) of the cells affect more the SS. The forward scatter threshold was set up to 15,000 events; this means that some debris and instrument noise are ignored. The instrument is equipped with blue (488 nm) and red (638 nm) excitation lasers and four emission filters (Table 2). The data were displayed using density dots for two parameters using a bivariate histogram, or cytogram (C), where the dot density of a population of cells forms a specific shape called a region (Dubelaar and Jonker 2000). A region can be drawn using a fluorescence parameter to define the population of interest (signature), or a region can be used to limit the cells that are drawn on a light scatterplot (gate).

Table 2 Naturally occurring fluorescent pigments in phytoplankton and their detection on the BD Accuri C6

Pigments	Excitation (nm)	Emission (nm)	C6 Detector (filter)
Chlorophyll a, b	488	>640 nm	FL3 (670 LP)
Phycoerythrin	488	575 nm	FL2 (585±20)
Phycocyanin	640	650 nm	FL4 (675±12.5)
Allophycocyanin	640	646 nm	FL4 (675±12.5)

A manual gate was drawn around the cell population on a plot of chlorophyll a fluorescence (FL3; 488 nm excitation, 640 nm emission) versus phycocyanin fluorescence (FL4; 640 nm excitation, 650 nm emission) and was used to discriminate and count the cells against volume calibrated fluidics.

Testing the concept of *Microcystis* removal by biofilter roots

To test for *Microcystis* cell removal by the biofilters (roots of living plants), the mesocosm experiments were conducted under different continuous flow conditions. At high flow (54 ± 3.0 cm^3 min^{-1}) with biofilters and synthetic fabric1 and fabric2. Fabric2 had higher packing density and was used as positive control with units as negative controls. At low flow (1.3 ± 0.2 cm^3 min^{-1}), the design included biofilters, one type of synthetic fabric (fabric1) and negative controls. The two flow conditions and three filter media treatment were each run in triplicates (Fig. 2).

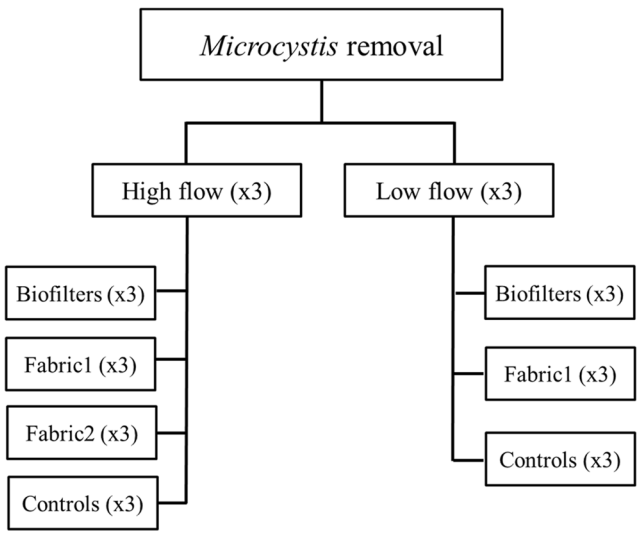

Fig. 2 Schematic of the experimental mesocosm design at two flow conditions for biofilters, synthetic fabrics (fabric1 and fabric2) and controls (× 3 = triplicates)

Prior to starting each of the experiments (high and low flow), the filtration units were filled with dechlorinated water and were left to stabilize for 2–3 h (high flow) and 48 h (low flow). The outflow was calibrated to 54 ± 3.0 cm^3 min^{-1} and 1.3 ± 0.2 cm^3 min^{-1} for high and low flow, respectively. Replicates of the experiment were run for 5, 7, and 11 days, which corresponded to two, three, and approximately five hydraulic retention times. A 12w LED submersible lamp with blue-red-white emission 400–700 nm, 800 lx providing approximately 20.6 μmol photons m^{-2} s^{-1}, was introduced into the feed tank after being thoroughly disinfected with 1 ppm chlorine solution and rinsed with sterilized (autoclaved) deionized water for the 11-day run experiments. The high flow experiments ran for 5 h.

Daily sampling (1 cm^3) was carried out for the low flow experiment at the sampling points shown in Fig. 1: feed tank (× 3); sampling points A (× 1), B (× 3) (depths 1, 5, and 9 cm), and C (× 1) for each filtration unit. Samples were taken every 55 min from the feed tank (× 3), A and B (× 1).

Removal efficiency

Removal efficiency as a percentage (RE%) was calculated for every paired inflow-outflow sample taken from the filtration units. This parameter is calculated with the assumption of a similar inlet and outlet flow rate (Eq. (4))

$$\%\mathrm{RE} = \frac{(C_0 - C)}{C_0} \times 100 \quad (4)$$

where C_0 is the concentration of *Microcystis* cells at the inlet and C is at the outlet.

Data processing and statistical analysis

Derived variables (ratio, percentages, and rates) and exploratory statistical analysis were undertaken using Excel (Microsoft © 2010) and SPSS v. 22 software. Data were transformed to meet the normal distribution and other parametric assumptions, and if assumptions could not be met, non-parametric tests were used. The non-parametric Friedman's test was applied to find differences between treatments and the Wilcoxon sign-rank test was applied to test for differences in the number of *Microcystis* cells in the unit's inflow and outflow.

Investigating chemical mechanisms: allelopathy

Further experimental work was required to understand what quantitative and qualitative mechanisms were taking place during the low flow experiments and determine if filtration alone or in combination with allelopathy was contributing to the removal of cells in the biofilters (Hilt and Gross 2008; Rojo et al. 2013). Two composite root exudate samples (from three biofilters) were screened and analyzed using gas chromatography coupled with mass spectrometry (GC-MS) to identify potential allelochemical compounds at Wessex Water Scientific Centre, Bath, UK, a United Kingdom Accredited Systems laboratory.

High-pressure liquid chromatography: sample preparation and analysis

To identify allelochemicals in the root exudate and root extraction from biofilters, a new method was developed using high-pressure liquid chromatography (HPLC) at Wessex Water Scientific Centre. Six chemical compounds (anthraquinone, gallic acid, gramine, hordenine, 4-5 indole-aldehyde, and stigmasterol) were purchased from Sigma-Aldrich. These compounds are known to be produced by *Phalaris arundinacea* and were selected based on their algaecide/algastatic properties against cyanobacteria and micro-algae (Hong et al. 2009; Xie et al. 2014; Shao et al. 2013). The compounds were used as standards, and all the stock solutions were prepared at 1 mg L^{-1} concentration in methanol. Individual (1:100) and a mix standard (6:100) in ultrapure water (UPW) solutions were prepared for extraction. Root exudate samples of 100 cm^3 taken from each biofilter were concentrated by a solid-phase extraction (SPE) step using a Visiprep (Supelco™ – Sigma-Aldrich). Roots of three plants were cut coarsely with a blender, adding 100 cm^3 of 30% methanol in deionized water (MilliQPore system) and concentrated by SPE. All samples were eluted from the cartridges with 1 cm^3 of 1% formic acid in methanol; the extracts were air dried (0.8 L min^{-1}) using a Visidry (Supelco – Sigma-Aldrich); and the dried residue was resuspended with 1 cm^3 10% acetonitrile: 0.1% acetic acid in ultrapure water (UPW).

An Agilent 1200 LC series system was used with UV/Vis-DAD detector. A HPLC Agilent column (C18, 150 mm × 5 mm) was used to achieve separation with a gradient elution consisting of acidified (acetic acid) acetonitrile:acidified (acetic acid) water (95:5). Column temperature was maintained at 40 °C and total run time was 45 min. The UV/Vis absorbance detector collected data at three wavelengths 205, 250, and 280 nm. Peak identity was validated through the use of retention times of external non-extracted and extracted standards with their respective spectrums All samples were kept at 5 °C at all times.

Results

Microcystis cell removal during high flow rate experiment

The packing densities of the synthetic filters with fibrous media were 0.03 for fabric1 and 0.07 for fabric2. The estimated

packing density of the biofilters was 0.05. The cumulative mass fraction of biofilters and fabric2 was ≤ 1 with the inflowing cell concentration, suggesting the system operates in deposition filtration mode for both types of fibrous media (Fig. 3A). The biofilter removal efficiency (RE%) of *Microcystis* cells is presented in Fig. 3B.

Microcystis cells were effectively removed from the biofilters and fabric2 (higher packing density) as shown by the decrease in numbers when comparing cell numbers from the outflow to the inflow (Wilcoxon sign test $T = 8$, $z = -4.34$, $p < 0.5$, $r = -0.47$ for biofilter and $T = 5$, $z = -0.46$, $p < 0.5$, $r = -0.47$ for fabric2).

Microcystis cell removal during low flow rate experiments

Results for *Microcystis* removal shown in Fig. 4 correspond to the experimental run of five hydraulic retention time (5 HRT). The biofilter cumulative mass fraction was > 1 at 4HRT before dropping rapidly (Fig. 4A). Fabric1 results shown are from the run of 3HRT (Fig. 4B). The biofilters showed removal efficiency of 40–55% within the first 3 days, dropping to 10–20%; after 3 days, RE for fabric1 was 8–20% (Fig. 4B).

Colour change in the units with biofilters, fabric, and the controls was observed. Results are shown for the biofilters and controls in Fig. 5A, B. The water in the biofilters is colourless, indicating the visual absence of *Microcystis* cells, whilst the fabric units and controls appear green, rich with cells. The same qualitative pattern was observed for all replicates of the experiment at low flow (run at 2 HRT and 3 HRT (× 2)).

Quantification of *Microcystis* cells (by flow cytometry) was four and a half times higher in the controls and fabric1 (low packing density) when compared to the biofilters. The number of cells from the feed tank increased every 48–72 h (results not shown) suggesting cell growth and conditions in the tank adequate for survival. By contrast, the number of cells in the biofilters remained at $1 \times 10^6 \pm 2 \times 10^5$ ml^{-1} from day 5 onwards (Fig. 5A). Comparative results between controls and biofilters are considered only until day 9 because a slight decline of *Microcystis* cells was observed in the controls after this day.

Significant differences in cell numbers were found between the inflow and outflow in the biofilters, with higher counts in the inflow than in the outflow (Wilcoxon sign test $T = 5$, $z = -5.164$, $p < 0.05$, $r = -0.53$). No significant differences in the number of *Microcystis* cells were found in the controls.

Investigating chemical mechanisms of *Microcystis* removal by biofilters

Allelochemical presence and HPLC-UV/Vis-DAD

Allelochemicals (i.e. phenols) and other secondary metabolites (i.e. cholesterol) were found in the screened samples. Table 3 shows the identified compounds with the GC-MS screening from the root exudate samples.

Standards with their respective retention times from the developed method to identify allelochemicals by HPLC-UV/Vis-DAD are shown in Table 4.

Table 5 compiles the identified compounds: gramine and 4-nitroindol-5-carboxaldehyde. Hordenine could not be traced in the mixed standard sample.

Figure 6 shows the chromatogram of a root exudate sample and root extracted sample. There are a large number of unidentified compounds in the samples. Spectrums of the unidentified peaks and their retention times might be compatible with phenolic compounds.

Discussion

Microcystis is a known bloom-forming cyanobacteria found worldwide in surface water reservoirs, and there has been increasing interest in eco-biological/rhizofiltration systems for its removal. The purpose of this study was to investigate whether *Microcystis* cells could be removed by the roots of *Phalaris arundinacea* under continuous flows and to establish the interactions between inflowing *Microcystis* cells with

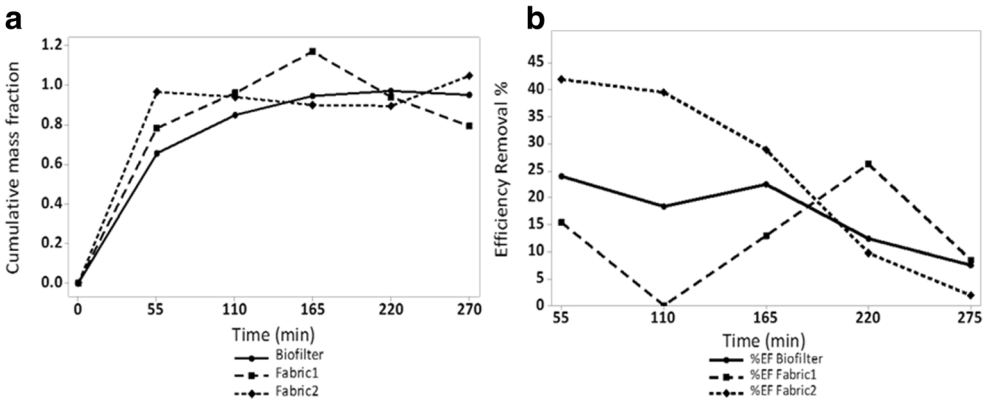

Fig. 3 (A) Cumulative mass fraction: biofilters (solid line); fabric1 (dashed line), and fabric2 (dotted line) as a function of time (min). (B) Removal efficiency (%) of *Microcystis* cells by the filter media in relation to hydraulic retention time (min)

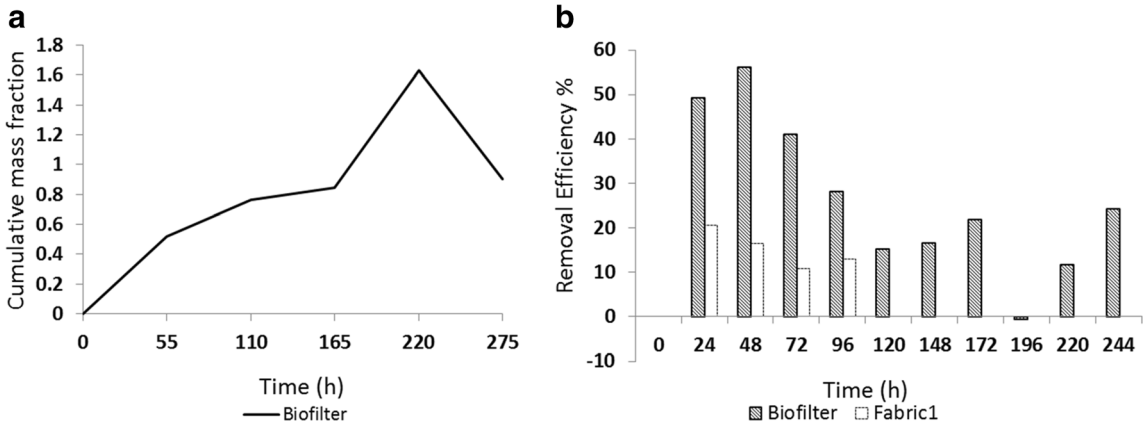

Fig. 4 (A) The cumulative mass fraction for the biofilters (solid line as a function of time (hours) equivalent to hydraulic retention time. (B) Removal efficiency (%) of *Microcystis* cells by the biofilter in relation to time (hours)

biofilters and synthetic filters. The distribution of the cells/compounds generated in the experimental system is known to be affected by hydrological processes (Alcocer et al. 2012; Ruggeri and Sassi 1993). Although it is assumed a system will reach steady-state in hydraulic-biochemically mediated processes, steady-state is rarely achieved in either plug-flow or continuously stirred systems (Potier et al. 2005). At water or sewage treatment plants, where it is very difficult to predict the load and environmental changes, the system typically does not reach equilibrium (Davis and Cornwell 2013). The system studied in this research did not reach steady-state within the experimental period.

Microcystis cell removal during the high flow experiment

Microcystis cell behaviour (as suspended particles) in relation to natural and synthetic media (natural and synthetic) suggests

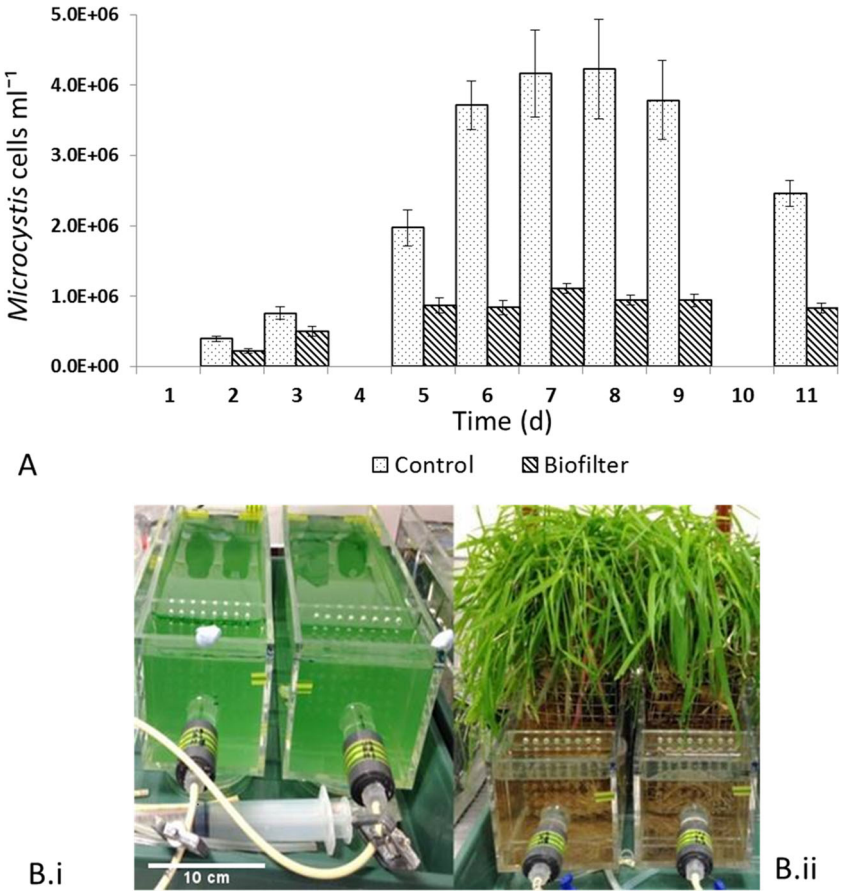

Fig. 5 (A) Quantitative changes in *Microcystis* average concentration (#cells ml^{-1}) for a mesocosm experiment run for 11 days or 5HRT. Controls (stipple), biofilters (striped), number of samples is $n = 3$ for each day. Error bars represent standard errors. (B) Qualitative changes in colouration: green control units (B.i) indicating the presence of *Microcystis* cells versus colourless biofiltration units (B.ii)

Table 3 GC-MS screening results of water samples from the filter units

Chemical identified	Concentration (ng dm^{-3})
Stigmasterol	660
Phenols	620
Salicylates	440
Cholesterol	250
β-cyclocitral	220

a deposition filtration mode or cumulative mass fraction (CMF = 1) (Fig. 3A). Differences in the cumulative mass fraction at different retention times initially showed the cells through the biofilters reach CMF = 1 at 220 min compared to fabric1, where CMF = 1 at 55 min. For removal efficiency, the biofilters were capable of removing 20–25% of the *Microcystis* cells during three retention times. The most effective filter media was fabric2 (synthetic filter with higher packing density than the biofilters and fabric1) with a maximum removal efficiency (%) slightly above 40% compared to 25% for the biofilters and to 17% for fabric1 at 55 min. These results show that there is a physical removal mechanism of the *Microcystis* cells by the biofilters, which can be related to packing density.

Microcystis cell removal during the low flow experiment

In the higher contact time experiment (i.e. low flow), the biofilters showed removal efficiencies twice as high as those observed under high flow conditions, suggesting that the increased exposure to the hydroponic rhizofiltration may contribute to higher removal efficiencies. At lower flow rates, the cell numbers in the feed tank doubled between 48 and 72 h, following a growth curve. A Growth Model fitted to the cell number data in the feed tank explained 95% of the variance of the data (results not shown). This growth could also have affected results for the CMF (Fig. 4A), as an increasing cell concentration would directly affect the ratios. The number of cells in the controls $\geq 3.0 \times 10^6$ cells ml^{-1} was at least twice as high as in the biofilters where they did not increase above 1.2×10^6 cells ml^{-1} (Fig. 5A). Hence, it was postulated that besides the physical removal, chemical mechanisms may contribute to the removal of *Microcystis* when exposed to biofilters, i.e. rhizofiltration.

The role of the biofilters on *Microcystis* removal

The most striking results found were the loss of colouration (bleaching) and the reduction in cell number in the biofilters when compared to the control and fabric units. "Bleaching" or chlorosis is defined in the literature as the change in pigmentation from blue-green to yellow-green to yellow (or orange) (Collier and Grossman 1992; Baier et al. 2014) in non-N_2 fixing cyanobacteria (like *Microcystis*) under nitrogen starvation conditions. Chlorosis is a process generally described after 72 h of nitrogen starvation in cultures of cyanobacteria model organisms such as *Synechocystis* and *Synechococcus* (Krasikov et al. 2012). However, there is no reference in the literature to the chlorotic process as a complete lack of colouration (clear as tap water) as observed in the biofilters (Fig. 5). The chlorotic process of *Microcystis* in the biofilters is observed after 72 h, and at 96 h there is a total absence of colouration with no-absorbance spectrophotometric detection at $O.D_{620}$ and $O.D_{680}$ (results not shown). Dagnino et al. (2006) described a chlorotic process in nutrient-depleted *Microcystis* cultures which after 3–5 days showed lack of colouration, but from blue-green to very pale blue-green and decreasing cell density. They attributed this phenomenon to intercellular signalling present in the medium of the nutrient-starved *Microcystis*. Intercellular signalling is a chemically mediated process between microorganisms (e.g. cyanobacteria and algae/organisms of higher taxa) known as allelopathy (Gross 2003). In this study, decrease in cell numbers was also seen, measured, and compared between the biofilters and the controls. These results suggest that either nutrient competition between the roots in the biofilters and *Microcystis* cells or allelochemical mechanisms with inhibiting/biocide effects (or both) induced chlorosis in the *Microcystis* cells. It is important to point out that the *Microcystis* cells were continuously injected to all the units in increasing concentration, but the only units with loss of colouration or reduction in cell numbers were the biofilters.

Table 4 Limits of detection and quantification for the selected analytes

Analytes from standard solution	Limit of detection (μg L^{-1})	Limit of quantification (μg L^{-1})
Hordenine	3.63	11.01
Gramine	13.46	40.78
Naringin	9.11	38.86
4-nitroindole-5-carboxaldehyde	14.83	44.93
Anthraquinone	29.20	88.48

Table 5 Allelochemicals quantified in root exudates and root extracts ($n = 3$)

Allelochemicals	Root exudate mean±SE µg L^{-1}	Root extract mean±SE µg L^{-1}
Gramine		3447 ± 1043
Naringin (ISTD 100 µg L^{-1})	109.3 ± 9.9	4688 ± 1433
4-Nitroindol-5-carboxaldehyde	96.13 ± 10.1	176 ± 10.1

Investigating allelochemical in roots and root exudate

The results of this study suggest the chlorotic effect and reduction in *Microcystis* cell numbers in the biofilters could be triggered by allelopathy. Allelochemical compounds with potentially algistatic/algaecide effects (Laue et al. 2014) were identified in the root exudate at nanogram concentrations (Table 2). These results mimic natural aquatic environments, where the allelochemicals excreted by macrophytes are diluted in the surrounding water (Hilt and Gross 2008; Rojo et al. 2013), but still have a suppression effect on phytoplankton growth rates (Körner and Nicklisch 2002; Mulderij et al. 2007; Chang et al. 2011). In water, the distances between cells are crucial as the chemical information is transmitted by diffusion and advective laminar flow (Wolfe 2000). By contrast, laboratory experiments are generally carried out using *Microcystis* cells at concentrations of 1×10^5–1×10^6 µl in the presence of µg or mg concentrations of allelochemicals either extracted from the roots or supplied commercially to demonstrate their biocidal effect (Lürling and De Senerpont Domis 2013; Lürling and Va Oosterhout 2013). However, allelopathy might not be only produced by the roots as any bacteria and fungi present could be sources of allelopathic chemicals. Nevertheless, studies on the detection and identification of allelochemicals in root tissue or root exudate from *Phalaris* spp. let alone *Phalaris arundinacea* have not been described in the literature.

The allelochemicals in the root exudate showed the presence of gramine and 4-nitroindol-5-carboxaldehyde with the targeted method developed for allelochemical detection (Fig. 6). However, there were additional unidentified compounds present in the root exudate and a large number in macerated root samples, which could potentially be released by the roots into the water. It is envisaged in future experiments to increase the number of allelochemicals in the mix standard to enable further identification. However, this does not mean that all compounds seen in the sample will have an algaecide/algistatic effect on *Microcystis*, and further investigation will be required to distinguish the impact of individual compounds on *Microcystis* cells.

Conclusions

Microcystis can be removed by the roots of *Phalaris arundinacea* under continuous flow conditions, but the mechanism could vary depending on residence time and packing density on synthetic/natural filter media. At higher residence

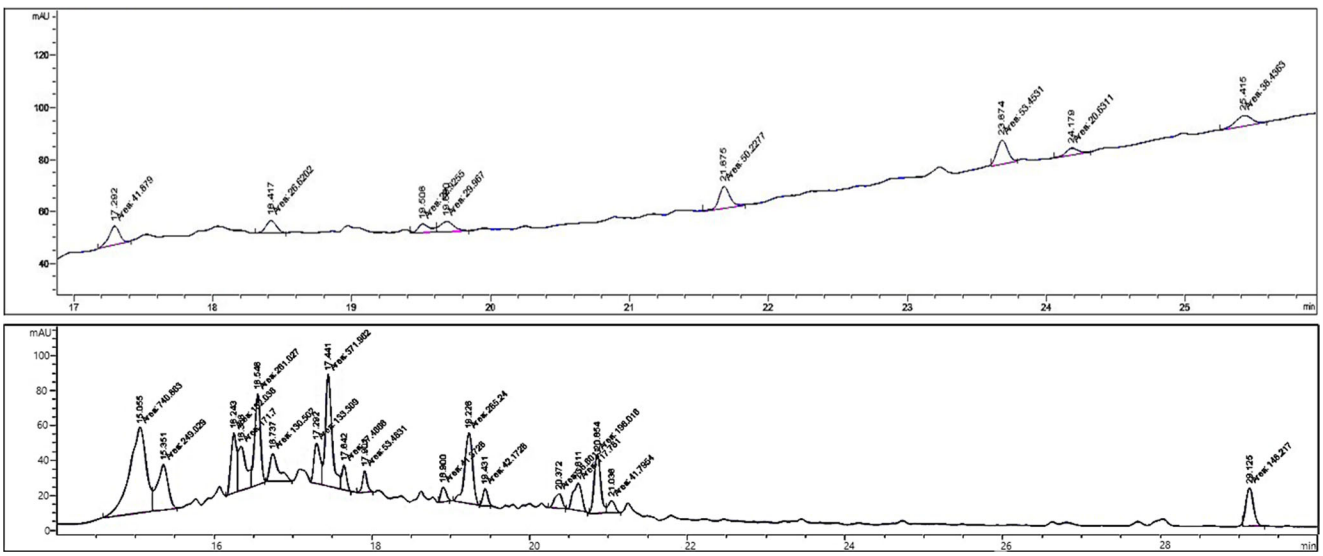

Fig. 6 Chromatograms of root exudate sample (top graph) and root extracted sample (bottom graph). These samples were from laboratory-grown *Phalaris*. The number of detected peaks for the exudate was eight and for the extract was 20

times on natural filter media, the decrease in *Microcystis* cell numbers is accompanied by a chlorotic process, indicating physicochemical mechanisms operate in natural filters compared to high flow where physical deposition was the main removal mechanism. This highlights the importance of creating pilot/field-scale designs to allow low flow velocities and/or large retention times, and increasing the probability of contact between the allelochemicals produced by the roots and the *Microcystis* cells.

Overall, at low residence time, it was shown that the packing density of the filter porous media plays the dominant role in *Microcystis aeruginosa 1450/3* removal in both biofilters and synthetic filter media. The packing density is a relevant factor to be considered in future Living-Filter systems if these are to be used as a pre-treatment process for phytoplankton removal.

Physicochemical interactions between living roots and *Microcystis* in hydroponic and continuous flow conditions have not been described in the literature before. Findings from this experimental set-up are more realistic at demonstrating these physicochemical interactions providing grounds for further experimentation, either with other phytoplankton or other plant species. Additionally, the biofiltration set-up used in this study can be used to investigate and optimize the removal of pharmaceuticals by living roots.

Acknowledgements From Thames Water, the authors thank specially Dr. Paul Rutter for his support and Nick Sutherland for assisting with the experimental set-up logistics. Thanks to Helen Shapland and Kevin O'Reilly, Trace Organics laboratory, Scientific Centre, Wessex Water Ltd., for allowing us the use of their HPLC. The authors are especially grateful to Toni Hall, Alexander T. Jennings and Gary Hunt for their assistance with developing the HPLC allelochemicals method.

Authors' contributions Conceptualization, experimental design, methodology, material preparation, data collection, formal analysis, investigation, writing original draft, and reviewing and editing were performed by Ana T. Castro Castellon. Resources, experimental design, data analysis, and validation were performed by Daniel S. Read. Conceptualization and writing original draft: Yaldah Azimi and Jocelyne M.R. Hughes. Supervision, project administration and resources: Jocelyne M.R. Hughes, Nicholas P. Hankins, and Michael J. Chipps. Funding acquisition by Michael J. Chipps. All authors reviewed, commented, and edited on previous versions of the manuscript.

Funding This project was fully sponsored by Thames Water Utilities Ltd. The design of the study presented in this manuscript, collection, analysis, and interpretation of data, and writing the manuscript are the views of the authors. Lady Margaret Hall, University of Oxford sponsored attendance to conferences where aspects of this work were presented.

Data availability The datasets used and/or analyzed during the current study are available from the corresponding author on reasonable request.

Compliance with ethical standards

Ethics approval Not applicable.

Consent for publication Not applicable.

Competing interests The authors declare that they have no competing interests.

References

Alcocer DJR, Vallejos GG, Champagne P (2012) Assessment of the plug flow and dead volume ratios in a sub-surface horizontal-flow packed-bed reactor as a representative model of a sub-surface horizontal constructed wetland. Ecol Eng 40:18–26

Baier A, Winkler W, Korte T, Lockau W, Karradt A (2014) Degradation of Phycobilisomes in *Synechocystis* sp. PCC6803 evidence for essential formation of a NblA1/NblA2 heterodimer and its codegradation by a Clp protease comples. J Biol Chem 289(17): 11755–11766

Benton TG, Solan M, Travis JM, Sait SM (2007) Microcosm experiments can inform global ecological problems. Trends Ecol Evol 22:516–521

Campos LC, Su MFJ, Graham NJD, Smith SR (2002) Biomass development in slow sand filters. Water Res 36:4543–4551

Castro-Castellon AT, Chipps MJ, Hankins NP, Hughes JMR (2016) Lessons from the "Living-Filter": an in-reservoir floating treatment wetland for phytoplankton reduction prior to a water treatment works intake. Ecol Eng 95:839–851

Chang DW, Hsieh ML, Chen YM, Lie TF, Chang JS (2011) Kinetics of cell lysis for *Microcystis aeruginosa* and *Nitzschia palea* in the exposure to beta-cyclocitral. J Hazard Mater 185:1214–1220

Chorus I, Bartram J (1999) Toxic cyanobateria in water: a guide to their public health consequences, monitoring and management. World Health Organization, 440 p., E&FN Spon, London

Collier JL, Grossman AR (1992) Chlorosis induced by nutrient deprivation in *Synechococcus* sp. strain PCC 7942: not all bleaching is the same. J Bacteriol 174(14):4718–4726

Conn SJ, Hocking B, Dayod M, Xu B, Atham A, Henderson S, Aukett L, Conn V, Shearer MK, Fuentes S, Tyerman SD, Gilliham M (2013) Protocol: optimising hydroponic growth systems for nutritional and physiological analysis of Arabidopsis thaliana and other plants. Plant Methods 9(1):1–11

Dagnino D, De Abreu Meireles D, De Aquino Almeida JC (2006) Growth of nutrient-replete *Microcystis* PCC 7806 cultures is inhibited by an extracellular signal produced by chlorotic cultures. Environ Microbiol 8(1):30–36

Davis ML, Cornwell DA (2013) Introduction to Environmental Engineering. New York (US)

Dubelaar GBJ, Onker RR (2000) Flow cytometry as a tool for the study of phytoplankton. Sci Mar 64(2):135–156

Dushenkov V, Kumar PN, Motto H, Raskin I (1995) Rhizofiltration: the use of plants to remove heavy metals from aqueous streams. Environ Sci Technol 29:1239–1245

Fan J, Ho L, Hobson P, Brookes J (2013) Evaluating the effectiveness of copper sulphate, chlorine, potassium permanganate, hydrogen peroxide and ozone on cyanobacterial cell integrity. Water Res 47: 5153–5164

Faulwetter JL, Gagnon V, Sundberg C, Chazarenc F, Burr MD, Brisson J, Camper AK, Stein OR (2009) Microbial processes influencing performance of treatment wetlands: a review. Ecol Eng 35(6):987–1004

Flörke M, Schneider C, McDonald RI (2018) Water competition between cities and agriculture driven by climate change and urban growth. Nat Sustain 1(1):51

Ger KA, Hansson L-A, Lürling M (2014) Understanding cyanobacteria-zooplankton interactions in a more eutrophic world. Freshw Biol 59: 1783–1798

Gross EM (2003) Allelopathy of aquatic autotrophs. Crit Rev Plant Sci 22:313–339

Headley TR, Tanner CC (2012) Constructed wetlands with floating emergent macrophytes: an innovative stormwater treatment technology. Crit Rev Environ Sci Technol 42:2261–2310

Hilt S, Gross EM (2008) Can allelopathically active submerged macrophytes stabilise clear-water states in shallow lakes? Basic Appl Ecol 9:422–432

Hong Y, Hu HY, Xie X, Sakoda A, Sagehashi M, Li FM (2009) Gramine-induced growth inhibition, oxidative damage and antioxidant responses in freshwater cyanobacterium *Microcystis aeruginosa*. Aquat Toxicol 91:262–269

Hudnell KH (2010) The state of US freshwater harmful algal blooms assessments, policy and legislation. Toxicon, 55 (5), SI, 1024-1034

Huisman J, Codd GA, Paerl HW, Ibelings BW, Verspagen JM, Visser PM (2018) Cyanobacterial blooms. Nat Rev Microbiol 16(8):471

Imai H, Chang KH, Kusaba M, Nakano SI (2008) Temperature-dependent dominance of *Microcystis* (Cyanophyceae) species: *M. aeruginosa* and *M. wesenbergii*. J Plankton Res 31:171–178

Jancula D, Marsalek B (2011) Critical review of actually available chemical compounds for prevention and management of cyanobacterial blooms. Chemosphere 85:1415–1422

Körner S, Nicklisch A (2002) Allelopathic growth inhibition of selected phytoplankton species by submerged macrophytes1. J Phycol 38(5): 862–871

Krasikov V, Aguirre von Wobeser E, Dekker HL, Huisman J, Matthijs HC (2012) Time-series resolution of gradual nitrogen starvation and its impact on photosynthesis in the cyanobacterium *Synechocystis* PCC 6803. Physiol Plant 145(3):426–439

Kurzbaum E, Kirzhener F, Armon R (2012) Improvement of water quality using constructed wetland systems. Rev Environ Health 27(1): 59–64

Laue P, Bahrs H, Chakrabarti S, Steinberg CE (2014) Natural xenobiotics to prevent cyanobacterial and algal growth in freshwater: contrasting efficacy of tannic acid, gallic acid, and gramine. Chemosphere 104: 212–220

Le Moal M, Gascuel-Odoux C, Ménesguen A, Souchon Y, Étrillard C, Levain A, Moatar F, Pannard A, Souchu P, Lefebvre A, Pinay G (2019) Eutrophication: a new wine in an old bottle? Sci Total Environ 651:1–11

Lu H, Yuan Y, Campbell DE, Qin P, Cui L (2014) Integrated water quality, energy and economic evaluation of three bioremediation treatment systems for eutrophic water. Ecol Eng 69:244–254

Lürling M, De Senerpont Domis LN (2013) Predictability of plankton communities in an unpredictable world. Freshwat Biol 58:455–462

Lürling M, Va Oosterhout F (2013) Controlling eutrophication by combined bloom precipitation and sediment phosphorus inactivation. Water Res 47:6527–6537

Marchand L, Nsanganwimana F, Oustriere N, Grebenshchykova Z, Lizama-Allende K, Mench M (2014) Copper removal from water using a bio-rack system either unplanted or planted with *Phragmites australis*, *Juncus articulatus* and *Phalaris arundinacea*. Ecol Eng 64:291–300

Martinez Hernandez J, Lopez-Rodas V, Costas E (2009) Microcystins from tap water could be a risk factor for liver and colorectal cancer: a risk intensified by global change. Med Hypotheses 72(5):539–540

Mulderij G, Van Nes EH, Van Donk E (2007) Macrophyte–phytoplankton interactions: the relative importance of allelopathy versus other factors. Ecol Model 204(1):85–92

Murray D, Jefferson B, Jarvis P, Parsons SA (2010) Inhibition of three algae species using chemicals released from barley straw. Environ Technol 31(4):455–466

O'Neil JM, Davis TW, Burford MA, Gobler CJ (2012) The rise of harmful cyanobacteria blooms: the potential roles of eutrophication and climate change. Harmful Algae 14:313–334

Otten TG, Paerl HW (2015) Health effects of toxic cyanobacteria in US drinking and recreational waters: our current understanding and proposed direction. Curr Environ Health Rep 2(1):75–84

Potier O, Leclerc JP, Pons MN (2005) Influence of geometrical and operational parameters on the axial dispersion in an aerated channel reactor. Water Res 39(18):4454–4462

Qin B, Paerl HW, Brookes JD, Liu J, Jeppesen E, Zhu G, Zhang Y, Xu H, Shi K, Deng J (2019) Why Lake Taihu continues to be plagued with cyanobacterial blooms through 10 years (2007-2017) efforts? Sci Bull 64:354–356. https://doi.org/10.1016/j.scib.2019.02.008

Raskin I, Ensley BD (2000) Phytoremediation of toxic metals: using plants to clean up the environment. John Wiley & Sons, Chichester, p 304

Rippka R, Deruelles J, Waterbutry JB, Herdman M, Staner RY (1979) Generic assignments, strain histories, and properties of pure cultures of cyanobacteria. J Gen Microbiol 11(1):1–61

Rojo C, Segura M, Rodrigo MA (2013) The allelopathic capacity of submerged macrophytes shapes the microalgal assemblages from a recently restored coastal wetland. Ecol Eng 58:149–155

Ruggeri B, Sassi G (1993) On the modelling approaches of biomass behaviour in bioreactor. Chem Eng Commun 122:1–56

Shao J, LIi R, Lepo JE Gu J-D (2013) Potential for control of harmful cyanobacterial blooms using biologically derived substances: Problems and prospects. J Environ Manag 125:149–155

U.S. EPA. 2005. Membrane filtration guidance manual, EPA 815-R-06-009. USEPA, Washington, DC

Vézie C, Rapala J, Vaitomaa J, Seitsonen J, Sivonen K (2002) Effect of nitrogen and phosphorus on growth of toxic and nontoxic microcystis strains and on intracellular microcystin concentrations. Microb Ecol 43(4):443–454

Weiss P, Westbrook A, Weiss J, Gulliver J, Bierboer D (2014) Effect of water velocity on hydroponic phytoremediation of metals. Int J Phytoremediation 16:203–217

Wolfe GV (2000) The chemical defense ecology of marine unicellular plankton: constraints, mechanisms, and impacts. Biol Bull 198(2): 225–244

Xie L, Hanyu T, Futatsugi N, Komatsu M, Steinman AD Park HD (2014) Inhibitory effect of naringin on microcystin-LR uptake in the freshwater snail Sinotaia histrica. Environ Toxicol Pharmacol 38(2):430–437